

Manipulating the Electrolyte Medium to Favor Either One-Electron or Two-Electron Oxidation Pathways for (Fulvalendiyl)dirhodium Complexes

Ayman Nafady,[†] Teen T. Chin,[‡] and William E. Geiger^{*}

Department of Chemistry, University of Vermont, Burlington, Vermont 05405

Received December 29, 2005

The anodic oxidations of three compounds having two Rh-containing moieties linked by a fulvalendiyl (Fv) dianion have been studied in varying electrolyte media. Following the integrated approach to manipulation of solvents and supporting electrolytes (Barrière, F.; Geiger, W. E. *J. Am. Chem. Soc.*, in press), $\Delta E_{1/2}$ values ($\Delta E_{1/2} = E_{1/2}(2) - E_{1/2}(1)$) of the successive one-electron oxidations of the neutral compounds to the corresponding dications were altered to either favor or disfavor the disproportionation of the mixed-valent intermediate. In the cases of $\text{Rh}_2\text{Fv}(\text{CO})_4$ (**1**) and $\text{Rh}_2\text{Fv}(\text{CO})_2(\mu\text{-dppm})$ (**2**) [Fv = C_{10}H_8 , dppm = bis(diphenylphosphino)methane], replacing the $[\text{PF}_6]^-$ supporting electrolyte anion with $[\text{B}(\text{C}_6\text{F}_5)]^-$ in CH_2Cl_2 changed the voltammograms from those of a single two-electron wave (having “inverted” $E_{1/2}$ potentials) to those of two distinct “normal” one-electron waves. In the case of $\text{Rh}_2\text{Fv}(\text{COD})_2$ (**3**, COD = C_8H_{12}), both the solvent and supporting electrolyte were changed to manipulate $\Delta E_{1/2}$ between normal and inverted values. Changes of up to 330 mV in $\Delta E_{1/2}$ were observed, resulting in modifications of over 10^5 in the disproportionation equilibrium constant, K_{disp} , of the mixed-valent intermediate $\mathbf{3}^+$. The thermodynamic stabilization of $\mathbf{1}^+$ and $\mathbf{2}^+$ allowed for their IR characterization and confirmed the previously postulated formation of Rh–Rh bonds in the cation radicals. An integrated approach to medium effects is shown to be a powerful method for manipulating the equilibrium concentrations of the various redox states that make up a multiple-electron-transfer process.

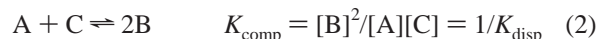
Introduction

Multistep electron-transfer processes are central to many aspects of redox chemistry.¹ In the conceptually simple case of two one-electron processes (an EE mechanism, written as successive oxidations of compound A in eq 1) the value of $\Delta E_{1/2}$ determines the equilibrium concentration of the one-electron intermediate B.



Since, in the great majority of cases, the $\Delta E_{1/2}$ value for two successive oxidations is positive,² the comproportionation

reaction of eq 2 is normally favored, B is thermodynamically stable with respect to the reverse (disproportionation) reaction,



and voltammetric scans show two separate one-electron waves.^{2d,e} For the much less common case of a negative $\Delta E_{1/2}$, which has been referred to as involving “inversion” of the normal ordering of $E_{1/2}(1)$ and $E_{1/2}(2)$,^{2d} a single two-electron wave may be observed, and the one-electron product B exists only in low equilibrium concentrations. Owing to differences in the physical and chemical properties of B compared to A and C, eq 2 may have a profound influence on the overall redox process, especially if B is a radical.

A number of electronic and structural factors are known to favor naturally compressed (i.e., small positive or negative) values of $\Delta E_{1/2}$.^{2d,3} In such cases, it may be possible to invert the potential ordering through changes in the medium. Solvent variations have been used to this end, for example, in the oxidation of tetraaryl-substituted ethylenes⁴ and in the reduction of transition metal clusters.⁵ Manipulation of $\Delta E_{1/2}$ values

* To whom correspondence should be addressed. E-mail: William.Geiger@uvm.edu.

[†] Present address: School of Chemistry, Monash University, Clayton, Victoria 3800, Australia.

[‡] Present address: ALS Technichem, Malaysia.

(1) For leading references see: (a) Bard, A. J. *Pure Appl. Chem.* **1971**, 25, 379. (b) Lowe, D. J.; Fisher, K.; Thomeley, R. N. F.; Vaughn, S.; Burgess, B. K. *Biochemistry* **1989**, 28, 8460. (c) Anson, F. C.; Shi, C.; Steiger, B. *Acc. Chem. Res.* **1997**, 30, 437. (d) Evans, D. H. *Acta Chem. Scand.* **1999**, 53, 876. (e) Bryce, M. R.; Batsanov, A. S.; Finn, T.; Hansen, T. K.; Howard, J. A. K.; Kamenjicki, M.; Lednev, I. K.; Asher, S. A. *J. Chem. Soc., Chem. Commun.* **2000**, 295. (f) Hapiot, P.; Kispert, L. D.; Konovalov, V. V.; Savéant, J.-M. *J. Am. Chem. Soc.* **2001**, 123, 6669. (g) Gileadi, E. *J. Electroanal. Chem.* **2002**, 532, 181. (h) Yandulov, D. V.; Schrock, R. R. *Science* **2003**, 76, 301.

(2) (a) Polcyn, D. S.; Shain, I. *Anal. Chem.* **1966**, 38, 370. (b) Richardson, D. E.; Taube, H. *Coord. Chem. Rev.* **1984**, 60, 107. (c) Pierce, D. T.; Geiger, W. E. *J. Am. Chem. Soc.* **1992**, 114, 6063. (d) Evans, D. H.; Lehmann, M. W. *Acta Chem. Scand.* **1999**, 53, 765. (e) Geiger, W. E. In *Laboratory Techniques in Electroanalytical Chemistry*, 2nd ed.; Kissinger, P. T., Heineman, W. R., Eds.; Marcel Dekker: New York, 1996; pp 698–700. (f) Bard, A. J.; Faulkner, L. R. *Electrochemical Methods*, 2nd ed.; John Wiley and Sons: New York, 2001; pp 243–247.

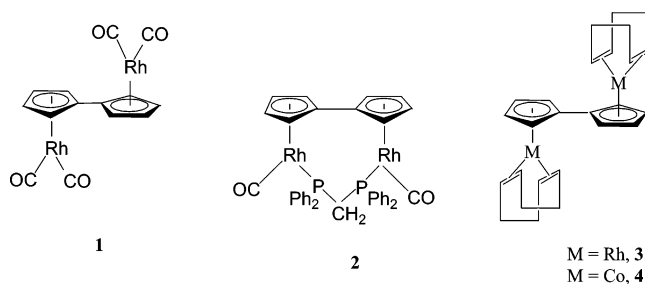
(3) (a) Creutz, C. In *Progress in Inorganic Chemistry*; Lippard, S. J., Ed.; John Wiley and Sons: New York, 1983; Vol. 30, p 1. (b) Ward, M. D. *Chem. Soc. Rev.* **1995**, 121. (c) Astruc, D. *Acc. Chem. Res.* **1997**, 30, 383. (d) Dümmeling, S.; Speiser, B.; Kuhn, N.; Weyers, G. *Acta Chem. Scand.* **1999**, 53, 876. (e) Baik, M.-H.; Ziegler, T.; Schauer, C. K. *J. Am. Chem. Soc.* **2000**, 122, 9143. (f) Lehmann, M. H.; Singh, P.; Evans, D. H. *J. Electroanal. Chem.* **2003**, 549, 137.

(4) (a) Svanholm, U.; Svensmark, B.; Parker, V. D. *J. Chem. Soc., Perkin Trans. 2* **1974**, 907. (b) Phelps, J.; Bard, A. J. *J. Electroanal. Chem.* **1976**, 68, 313. (c) Rathore, R.; Lindeman, S. V.; Kumar, A. S.; Kochi, J. K. *J. Am. Chem. Soc.* **1998**, 120, 6931.

(5) Jund, R.; Rimmelin, J.; Gross, M. *J. Organomet. Chem.* **1990**, 381, 239.

through ion-pairing effects are more widely known. For example, with cathodic processes involving *product anions*, the one-electron product is thermodynamically destabilized under stronger ion-pairing conditions typified by replacement of tetraalkylammonium ions by alkali metal ions.⁶ An essentially “mirror image” effect⁷ is expected for anodic processes involving *product cations* if “traditional” anions such as $[\text{PF}_6]^-$ ⁸ are replaced by strong ion-pairing anions such as halide ions. However, the greatly increased nucleophilicities of the latter often lead to unwanted side reactions. A new expedient to this strategy has been recently introduced. Weakly coordinating anions (WCA)⁹ having highly dispersed negative charges (e.g., $[\text{B}(\text{C}_6\text{F}_5)_4]^-$, TFAB,^{10–12} and $[\text{B}(\text{C}_6\text{H}_3(\text{CF}_3)_2)_4]^-$, BArF_{24} ¹³) provide the desired weak nucleophilicity in addition to being much more weakly ion-pairing than the traditional anions in low-polarity solvents.¹² These properties make possible the manipulation of anodic $\Delta E_{1/2}$ values by ion-pairing effects with little concern about nucleophile-induced follow-up reactions. A systematic study of media containing halide, traditional, or weakly coordinating anions has provided an integrated model for the manipulation of $\Delta E_{1/2}$ values in lower-polarity solvents.^{7,11} Here we give an example of how this integrated approach to medium effects makes possible either two separate one-electron processes or a single (inverted) two-electron process for the oxidation of compounds having a fulvalene-type bridge between two Rh atoms.

Two of these complexes, namely, $\text{Rh}_2\text{Fv}(\text{CO})_4$, **1**, and $\text{Rh}_2\text{Fv}(\text{CO})_2(\mu\text{-dppm})$, **2** [Fv = fulvalenediyl, C_{10}H_8 ; dppm = bis(diphenylphosphino)methane], were shown earlier to have *single two-electron* oxidations¹⁴ in which potential inversion is linked to formation of strong Rh–Rh bonds in the dications. In neither case was the radical monocation (**1**⁺ or **2**⁺) detected, hindering judgment on the question of whether the metal–metal bond forms in the first or second oxidation process. The fact that the reported values¹⁴ of $\Delta E_{1/2}$ were not very large in $\text{CH}_2\text{Cl}_2/[\text{NBu}_4][\text{PF}_6]$ (–140 mV for **1** and –10 mV for **2**) suggested to us that these compounds might have *positive* $\Delta E_{1/2}$ values in less ion-pairing media, hopefully allowing direct characterization of the monocations **1**⁺ and **2**⁺. This expectation was realized by electrochemistry and spectroscopy, as shown below.



Experimental Section

General Procedures. The dirrhodium compounds **1–3** and the dicobalt compound **4** were prepared by literature methods.^{14,15} All procedures were carried out under dinitrogen using rigorous Schlenk conditions, except for electrochemical experiments, which were carried out in a Vacuum Atmospheres drybox. Dichloromethane was twice distilled from CaH_2 , the second time under static vacuum. Tetrabutylammonium hexafluorophosphate was prepared by metathesis of $[\text{NBu}_4]\text{I}$ with $[\text{NH}_4][\text{PF}_6]$ in acetone/water, recrystallized three times from ethanol, and dried under vacuum. $[\text{NBu}_4][\text{B}(\text{C}_6\text{F}_5)_4]$ was prepared by metathesis of $[\text{NBu}_4]\text{Br}$ with $\text{Li}[\text{B}(\text{C}_6\text{F}_5)_4]\cdot n\text{OEt}_2$ (Boulder Scientific Co.) in methanol and recrystallized at least twice from CH_2Cl_2 /hexane. A detailed description of the metathesis procedure is available.¹² $[\text{FeCp}_2][\text{B}(\text{C}_6\text{F}_5)_4]$ (Boulder Scientific Co.) was used as received. The tetraethylammonium and tetrabutylammonium salts of $[\text{B}(\text{C}_6\text{H}_3(\text{CF}_3)_2)_4]^-$ were prepared by similar metatheses and recrystallizations. $[\text{FeCp}_2][\text{B}(\text{C}_6\text{F}_5)_4]$ was prepared by oxidation of sublimed ferrocene with anhydrous FeCl_3 , followed by treatment with $\text{Li}[\text{B}(\text{C}_6\text{F}_5)_4]\cdot n\text{OEt}_2$, analogous to the literature preparation of the $[\text{PF}_6]^-$ analogue.^{16,17} A standard three-electrode configuration was used for voltammetry and coulometry experiments. In the case of bulk electrolyses a three-compartment cell was used in which the working and auxiliary compartments were separated by two fine frits to minimize mixing of the solutions. The experimental reference electrode was a AgCl -coated Ag wire prepared by anodic electrolysis of the wire in 1 M HCl . All potentials in this paper are referred, however, to the ferrocene/ferrocenium reference couple.¹⁶ This was accomplished by adding either ferrocene or decamethylferrocene to the solution as an internal standard at an appropriate time in the experiment. When decamethylferrocene was used as the working internal reference,

(6) Although ion-pairing shifts both the A/B and B/C couples to more positive potentials, the effect on the latter is stronger owing to the increased electrostatic effect in the dianion. Early work in this area is nicely summarized in (a) Swarc, M.; Jagur-Grodzinski, J. In *Ions and Ion Pairs in Organic Reactions*; Swarc, M., Ed.; John Wiley and Sons: New York, 1974; Vol. 2, Chapter 1. Other representative studies: (b) Levin, G.; Swarc, M. *J. Am. Chem. Soc.* **1976**, *98*, 4211. (c) Smith, W. H.; Bard, A. J. *J. Electroanal. Chem.* **1977**, *76*, 19 [cyclooctatetraene; see also ref 6f]. (d) Böhm, A.; Meerholz, K.; Heinze, J.; Müllen, K. *J. Am. Chem. Soc.* **1992**, *114*, 688 (polyarenes). (e) Himeno, S.; Takamoto, M.; Ueda, T. *J. Electroanal. Chem.* **2000**, *485*, 49 (keggin-type complexes). (f) Baik, M.-H.; Schauer, C. K.; Ziegler, T. *J. Am. Chem. Soc.* **2002**, *124*, 11167 (density functional theory of ion-pairing interactions). See also ref 2d.

(7) Barrière, F.; Geiger, W. E. *J. Am. Chem. Soc.*, in press. See ref 11 for preliminary communication of this work.

(8) We include in this category the anions most commonly used in nonaqueous solutions such as $[\text{BF}_4]^-$, $[\text{ClO}_4]^-$, and $[\text{CF}_3\text{SO}_3]^-$.

(9) (a) Beck, W.; Stükel, K. H. *Chem. Rev.* **1988**, *88*, 1405. (b) Strauss, S. H. *Chem. Rev.* **1993**, *93*, 927. (c) Reed, C. A. *Acc. Chem. Res.* **1998**, *31*, 133. (d) Chen, E. Y.-K.; Marks, T. J. *Chem. Rev.* **2000**, *100*, 1391. (e) Krossing, I.; Raabe, I. *Angew. Chem., Int. Ed.* **2004**, *43*, 2066.

(10) LeSuer, R. J.; Geiger, W. E. *Angew. Chem., Int. Ed.* **2000**, *38*, 248.

(11) Barrière, F.; Camire, N.; Geiger, W. E.; Mueller-Westerhoff, U. T.; Sanders, R. *J. Am. Chem. Soc.* **2002**, *124*, 7262.

(12) LeSuer, R. J.; Buttolph, C.; Geiger, W. E. *Anal. Chem.* **2004**, *76*, 6395.

(13) Hill, M. G.; Lamanna, W. M.; Mann, K. R. *Inorg. Chem.* **1991**, *30*, 4687.

(14) Chin, T. T.; Geiger, W. E.; Rheingold, A. L. *J. Am. Chem. Soc.* **1996**, *118*, 5002.

(15) Rausch, M. D.; Spink, W. C.; Conway, B. G.; Rogers, R. D.; Atwood, J. L. *J. Organomet. Chem.* **1990**, *383*, 227.

(16) (a) Gritzner, G.; Kuta, J. *Pure Appl. Chem.* **1984**, *56*, 461. (b) Connelly, N. G.; Geiger, W. E. *Chem. Rev.* **1996**, *96*, 877.

Table 1. $E_{1/2}$ Values (volt vs ferrocene) for Fulvalenyl Dirhodium Complexes in Dichloromethane, **1** = $\text{Rh}_2\text{Fv}(\text{CO})_4$, **2** = $\text{Rh}_2\text{Fv}(\text{CO})_2(\mu\text{-dppm})$ at RT (boldface indicates $\Delta E_{1/2}$ value having potential inversion; TFAB = $[\text{B}(\text{C}_6\text{F}_5)_4]^-$, $\text{BArF}_{24} = [\text{B}(\text{C}_6\text{H}_3(\text{CF}_3)_2)_4]^-$)

cmpd	med ^a	supporting electrolyte	$E_{1/2}(1)$	$E_{1/2}(2)$	$\Delta E_{1/2}$ (mV)	meas ^b
1	(i)	$[\text{NBu}_4][\text{TFAB}]$, 0.05 M	0.07	0.15	80	DPV ^c
1	(ii)	$[\text{NBu}_4][\text{BArF}_{24}]$, 0.05 M	0.08	0.17	90	DPV ^c
1	(iii)	$[\text{NEt}_4][\text{BArF}_{24}]$, 0.05 M	0.08	0.20	125	SWV
1	(iv)	$\text{Na}[\text{BArF}_{24}]$, 0.02 M	0.10	0.28	180	CV
1	(v)	$[\text{NBu}_4][\text{PF}_6]$, 0.1 M	(single wave, $E_{1/2} = -0.17$)		-140	CV _{sim} ^d
2	(vi)	$[\text{NBu}_4][\text{TFAB}]$, 0.1 M	-0.75	-0.65 ₅	95	DPV ^c
2	(ii)	$[\text{NBu}_4][\text{BArF}_{24}]$, 0.05 M	-0.74	-0.63 ₅	105	SWV
2	(iv)	$\text{Na}[\text{BArF}_{24}]$, 0.02 M	-0.76	-0.57 ₅	185	CV
2	(v)	$[\text{NBu}_4][\text{PF}_6]$, 0.1 M	(single wave, $E_{1/2} = -0.75$)		ca. -10	CV _{sim} ^d

^a Medium, numbered to help identify matches. ^b Voltammetric method used to determine $\Delta E_{1/2}$: DPV = differential pulse voltammetry; SW = square-wave voltammetry; CV = cyclic voltammetry; CV_{sim} = cyclic voltammetry digital simulations. ^c Single unresolved peak; $\Delta E_{1/2}$ determined from width of voltammogram at half-height. ^d In acetone: see ref 14.

adjustment to the ferrocene reference potential was made by adding 0.61 V if the medium was $\text{CH}_2\text{Cl}_2/0.1$ M $[\text{NBu}_4][\text{B}(\text{C}_6\text{F}_5)_4]$ or 0.55 V if the medium was $\text{CH}_2\text{Cl}_2/0.1$ M $[\text{NBu}_4][\text{PF}_6]$. The working electrodes were glassy carbon disks having a diameter of either 1 or 1.5 mm (Bioanalytical systems), polished on a Buehler polishing cloth with Metadi II diamond paste, rinsed copiously with Nanopure water, and placed under vacuum for drying. Bulk electrolyses were performed at Pt basket electrodes. Cyclic voltammetry (CV) scans were subjected to mechanistic diagnostics employing the procedures detailed elsewhere.¹⁸ Linear scan voltammetry (LSV) at a 2 mV s⁻¹ scan rate using a 1.5 mm diameter disk achieved quasi-steady-state conditions. A PARC model 273A potentiostat was employed, and digital simulations were carried out using Digisim 3.0 (Bioanalytical Systems). Temperatures were ambient unless otherwise noted.

The $\Delta E_{1/2}$ values were measured using one of three different voltammetric methods. Simple visualization of the CV peaks was satisfactory in many cases. Square-wave voltammetry (SWV, frequencies of 10 Hz or higher) and differential pulse voltammetry (DPV, pulse height 10 mV) were employed when the $|\Delta E_{1/2}|$ values were less than about 110 mV. If the two one-electron peaks were unresolved in DPV scans, the width of the voltammogram at half-height was used to obtain $\Delta E_{1/2}$.¹⁹ The precision of $\Delta E_{1/2}$ values given in this paper is believed to be 10 mV or better.

In-situ IR spectra were obtained on bulk electrolysis solutions using the fiber-optic transmission method previously described.^{20,21} In this method a "dip" probe is connected to an FTIR spectrometer (Mattson Polaris in this case) through a 1 m fiber-optic cable (Remspec Corp) and operated in an external reflectance mode at a gold surface using 4 cm⁻¹ resolution. A spectral window of ca. 1500 to 2200 cm⁻¹ was available for the electrolysis solutions employed in this study. ESR spectra were obtained with a Bruker ESP 300E spectrometer.

Results

I. Converting **1 and **2** to Separate One-Electron Anodic Processes.** As mentioned in the Introduction, with $[\text{PF}_6]^-$ as the electrolyte anion, compounds **1** and **2** have negative (i.e., inverted) $\Delta E_{1/2}$ values and display single two-electron quasi-reversible²² anodic waves²³ (eq 3). The thermodynamic instability

(17) For the preparation of other ferrocenium salts having fluorine-containing aryl borate counterions see: Calderazzo, F.; Pampaloni, G.; Rocchi, L.; Englert, U. *Organometallics* **1994**, *13*, 2592. For the structural characterization of $[\text{FeCp}_2][\text{TFAB}]$ prepared using $[\text{N}(\text{C}_6\text{H}_4\text{Br})_3][\text{TFAB}]$ as oxidant see: O'Connor, A. R.; Nataro, C.; Golen, J. A.; Rheingold, A. L. *J. Organomet. Chem.* **2004**, *689*, 2411.

(18) Geiger, W. E. In *Laboratory Techniques in Electroanalytical Chemistry*, 2nd ed.; Kissinger, P. T., Heineman, W. R., Eds.; Marcel Dekker: New York, 1996; Chapter 23.

(19) Richardson, D. E.; Taube, H. *Inorg. Chem.* **1981**, *20*, 1278.

(20) Shaw, M. J.; Geiger, W. E. *Organometallics* **1996**, *15*, 13.

(21) Stoll, M. E.; Geiger, W. E. *Organometallics* **2004**, *23*, 5818.

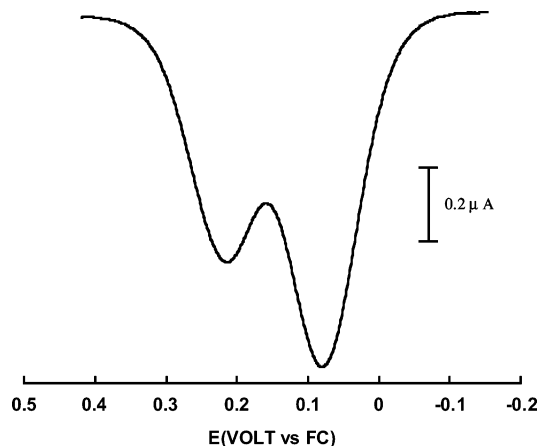
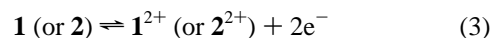


Figure 1. Differential-pulse voltammogram of 1 mM **1** in $\text{CH}_2\text{Cl}_2/0.05$ M $[\text{NEt}_4][\text{B}(\text{C}_6\text{H}_3(\text{CF}_3)_2)_4]$ at a pulse height of 10 mV, a scan rate of 2 mV s⁻¹, and a 1.5 mm GC disk electrode.

of the one-electron products precluded their spectroscopic characterization in earlier work.¹⁴



IA. Oxidation of **1.** Replacing the $[\text{PF}_6]^-$ anion by TFAB or BArF_{24} increases $\Delta E_{1/2}$ by preferentially decreasing ion-pairing to the product dications compared to the corresponding monocations. Positive values of $\Delta E_{1/2}$ are observed for **1** in four different electrolyte media, the highest value being 180 mV in $\text{CH}_2\text{Cl}_2/0.02$ M $\text{Na}[\text{BArF}_{24}]$ (electrolyte (iv), Table 1). The two one-electron waves are visually resolved in this electrolyte and in $\text{CH}_2\text{Cl}_2/0.05$ M $[\text{NEt}_4][\text{BArF}_{24}]$ (electrolyte (iii), Table 1, Figure 1). The closeness of the $\Delta E_{1/2}$ values with the two tetrabutylammonium salts of electrolytes (i) and (ii) are consistent with TFAB and BArF_{24} having very similar ion-pairing abilities in dichloromethane. It may at first seem surprising that still larger $\Delta E_{1/2}$ values were attained when the electrolyte counteraction was changed from $[\text{NBu}_4]^+$ ($\Delta E_{1/2} = 90$ mV) to $[\text{NEt}_4]^+$ (125 mV) or Na^+ (180 mV). This may be qualitatively understood^{7,24} as a secondary effect in which a more strongly ion-pairing electrolyte cation (e.g., Na^+) competes with the analyte cation for the electrolyte anion.

(22) "Quasi-reversible" refers to sluggish electron-transfer kinetics. Both oxidations are chemically reversible on the CV time scale. For a discussion of quasi-reversibility see ref 2f, pp 191–204.

(23) An added difficulty with oxidation of **1** was the insolubility of its oxidation products with $[\text{PF}_6]^-$ counterions. This precluded the use of dichloromethane and related low-donor solvents.

(24) Changes in electrolyte concentrations also influence the changes in these values. The available concentrations of $\text{Na}[\text{BArF}_{24}]$ were limited by its solubility in CH_2Cl_2 .

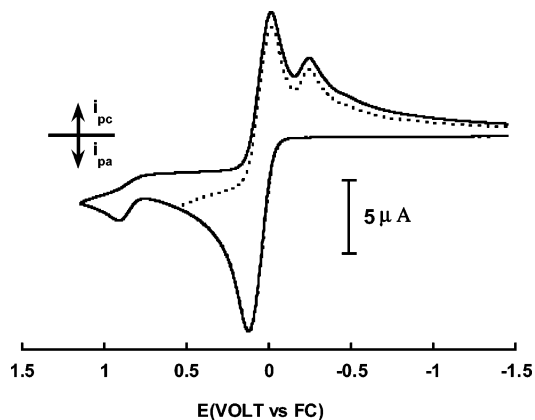


Figure 2. Cyclic voltammogram of 2 mM **1** in $\text{CH}_2\text{Cl}_2/0.05 \text{ M}$ $[\text{NBu}_4][\text{TFAB}]$ at a scan rate of 0.2 V s^{-1} , 1 mm GC disk electrode.

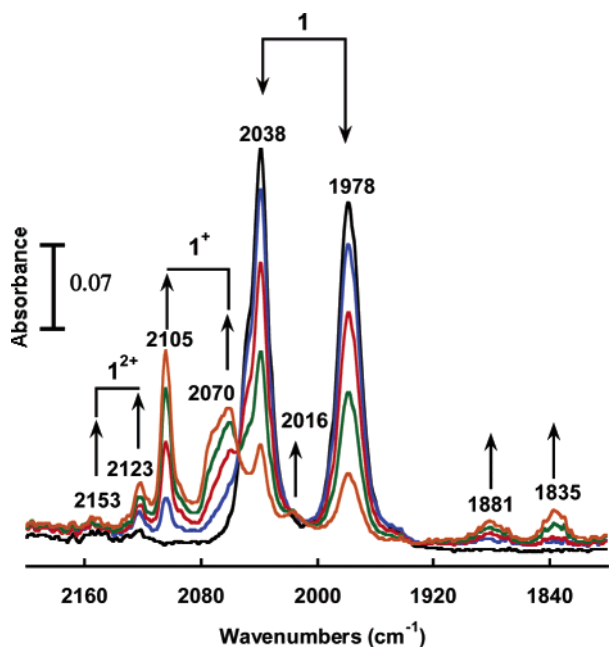
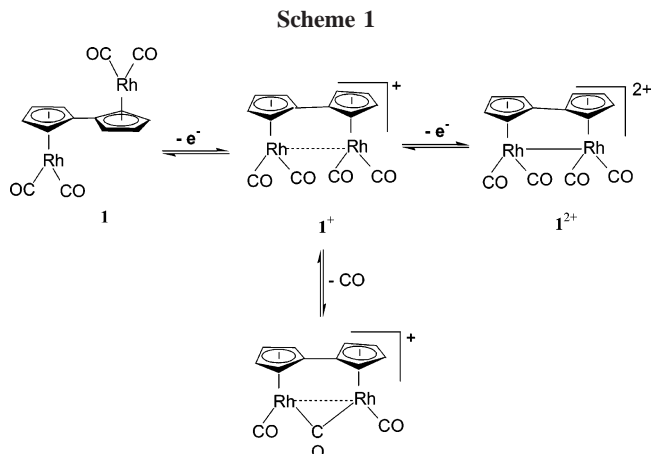


Figure 3. In-situ IR spectroelectrochemical monitoring of bulk oxidation of 1 mM **1** in $\text{CH}_2\text{Cl}_2/0.04 \text{ M}$ $[\text{NEt}_4][\text{B}(\text{C}_6\text{H}_3(\text{CF}_3)_2)_4]$ at $E_{\text{appl}} = 0.4 \text{ V vs Fc/Fc}^+$, 273 K.

Since the $\Delta E_{1/2}$ value of 125 mV with $[\text{NEt}_4][\text{BArF}_2\text{F}_4]$ was sufficiently large to promise a spectroscopically detectable equilibrium concentration of 1^+ , this electrolyte was used for one-electron anodic electrolyses of **1** in CH_2Cl_2 . A complication that must be noted here is that the oxidation of **1** is not completely chemically reversible,¹⁴ and even in WCA electrolytes some evidence of chemical follow-up products are seen in CV scans at room temperature (Figure 2). The fact that the follow-up reaction is not quenched by substitution of a WCA for $[\text{PF}_6]^-$ suggests that the kinetic instability of 1^+ arises from factors other than anionic nucleophilic attack, perhaps involving loss of CO.

Bulk electrolysis of **1** was carried out ($E_{\text{appl}} = 0.4 \text{ V}$, $T = 273 \text{ K}$) and in-situ IR spectra were recorded as the electrolysis proceeded. As shown in Figure 3, after passage of 0.85 F/equiv, the original pair of ν_{CO} bands at 2038 and 1978 cm^{-1} for **1** had largely disappeared, being replaced in the terminal CO region by two strong features [2105 and ca. 2070 cm^{-1} (broad)] and two weak features (2153 and 2123 cm^{-1}). Weak bands also develop in the bridging CO region at 1881 and 1835 cm^{-1} . Continuing the electrolysis to yet higher coulomb counts first resulted in near resolution of the ca. 2070 cm^{-1} feature into a



pair at 2073 and 2061 cm^{-1} , after which the second of these diminished along with the band at 2105 cm^{-1} as two new peaks at 2153 and 2123 cm^{-1} , known to be those of the dication 1^{2+} ,¹⁴ grew in. As expected, these last two bands became prominent upon completion of the electrolysis (1.35 F/equiv).²⁵ Three residual features remain, at 2073, 1881, and 1835 cm^{-1} . Because the most likely follow-up reaction of 1^+ is loss of CO, the bands at 2073 and 1881 cm^{-1} are tentatively assigned to singly bridged $[\text{Rh}_2\text{Fv}(\text{CO})_2(\mu\text{-CO})]^+$. Although the remaining feature at 1835 cm^{-1} falls at the same energy as that reported¹⁵ for the neutral complex $\text{Rh}_2\text{Fv}(\text{CO})_2(\mu\text{-CO})$, we do not observe a second band reported at 1979 cm^{-1} . Scheme 1 summarizes our understanding of the anodic reactions of **1**.

The most significant IR assignments are those made to 1^+ . The pair at 2105 and 2061 cm^{-1} are shifted by +67 and +83 cm^{-1} , respectively, from those of **1** and provide a strong argument for Rh–Rh bond formation in the monocation. Were this not to occur, one would expect *four* intense IR bands for 1^+ , including two close to the energies of the original pair for **1**.^{26,27} Strengthening this reasoning is the fact that the average shift of 75 cm^{-1} for $\Delta\nu_{\text{CO}}$ ($1/1^+$) is quite similar to that (84 cm^{-1}) observed for the Co analogues $[\text{Co}_2\text{Fv}(\text{CO})_4]^{0/+}$, in which Co–Co bond formation has been confirmed by ESR spectroscopy.²⁸

IB. Oxidation of 2. The oxidation chemistry of the dppm-bridged compound **2** has the advantage of not being complicated by homogeneous follow-up reactions, and the crystalline dication 2^{2+} is easily isolable. Analysis of the shape of the *single two-electron* CV waves for either **2** or 2^{2+} in $[\text{PF}_6]^-$ -containing media gave a $\Delta E_{1/2}$ value of ca. –10 mV.¹⁴ As shown in Table 1, significant positive increases in $\Delta E_{1/2}$ are achieved with WCA electrolytes, lowering the disproportionation constant for 2^+ by

(25) The fact that exhaustive electrolysis at $E_{\text{appl}} = 0.4 \text{ V}$ required significantly less than 2 F/equiv is further indication of the kinetic instability of the monocation 1^+ .

(26) Four bands are expected for two metal dicarbonyl fragments electronically coupled in a class II mixed-valent compound of the type expected if 1^+ had a *cisoid* structure. For examples see ref 27. We also note that a metal–metal bonded system may show one or more additional weak bands owing to weak vibrational coupling of the nonadjacent carbonyls [ref 27b]. This likely accounts for a third, weak, feature at 2016 cm^{-1} , which tracks the pair at 2105 and 2061 cm^{-1} and is also assigned to 1^+ (Table 2).

(27) (a) Pierce, D. T.; Geiger, W. E. *Inorg. Chem.* **1994**, *33*, 373. (b) Atwood, C. G.; Geiger, W. E. *J. Am. Chem. Soc.* **2000**, *122*, 5477. (c) Connelly, N. G.; Kelly, R. L.; Kitchen, M. D.; Mills, R. M.; Stansfield, R. F. D.; Whiting, S. M.; Woodward, P. *J. Chem. Soc., Dalton Trans.* **1981**, 1317.

(28) Spectra of the radical $[\text{Co}_2\text{Fv}(\text{CO})_4]^+$ have hyperfine splittings from two equivalent metals, $A_{\text{iso}} = 10 \text{ G}$, $A_{\text{II}} = 47 \text{ G}$, A_{I} ca. –8 G; Nafady, A., Geiger, W. E. Unpublished work at University of Vermont.

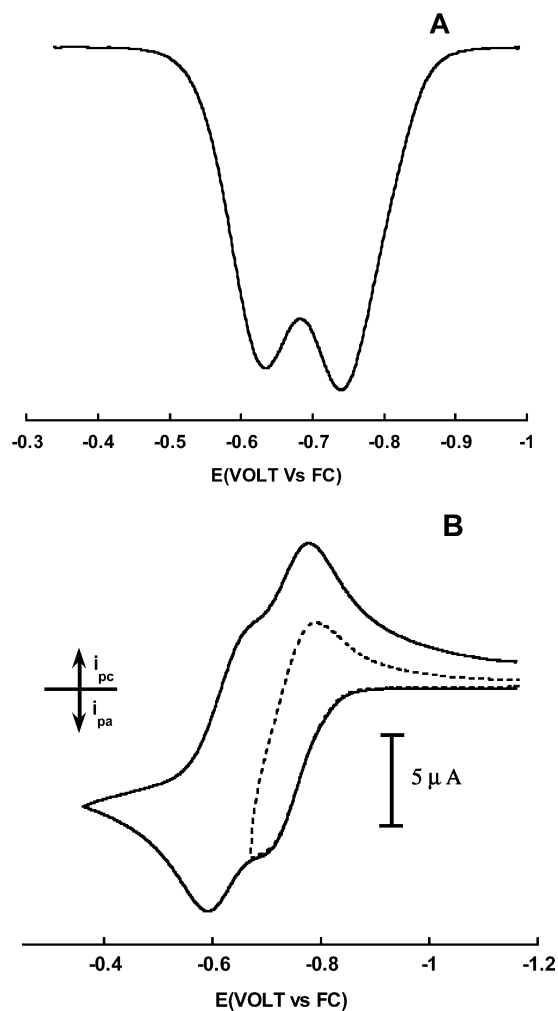


Figure 4. (A) Square-wave voltammogram of 1.6 mM **2** in $\text{CH}_2\text{Cl}_2/0.05\text{M} [\text{NBu}_4][\text{B}(\text{C}_6\text{H}_5(\text{CF}_3)_2)_4]$, 150 Hz, 1.5 mm GC electrode. (B) Cyclic voltammogram of **2** under the same conditions, scan rate 0.1 V s^{-1} .

a factor of about 10^3 (eq 4). Figure 4 has representative voltammograms showing the resolved one-electron waves.



Bulk electrolysis (at $E_{\text{appl}} = -0.5 \text{ V}$) and IR spectroelectrochemistry were carried out on a light red 0.5 mM solution of **2** in $\text{CH}_2\text{Cl}_2/0.05 \text{ M} [\text{NBu}_4][\text{TFAB}]$ at 273 K. As the electrolysis proceeded to virtual completion with passage of 0.93 F/quiv, the solution became a dark yellow-green as the original carbonyl band at 1942 cm^{-1} decreased (Figure 5, top) and a new prominent band grew in at 2024 cm^{-1} , which, along with the less intense band at 1992 cm^{-1} , is assigned to $\mathbf{2}^+$. The small absorbance at 2082 cm^{-1} , seen late in this sequence, arises from the dication $\mathbf{2}^{2+}$. These assignments were confirmed by the further electrolysis to $\mathbf{2}^{2+}$ (an additional 0.92 F/quiv was released as the solution became yellow), during which the 2024 and 1992 cm^{-1} bands were replaced by the pair at 2082 and 2054 cm^{-1} (Figure 5B) previously ascribed to $\mathbf{2}^{2+}$.¹⁴

The IR results are qualitatively consistent with the voltammetry data in that the disproportionation reaction of eq 4 is shown to be weighted in favor of $\mathbf{2}^+$ under these conditions

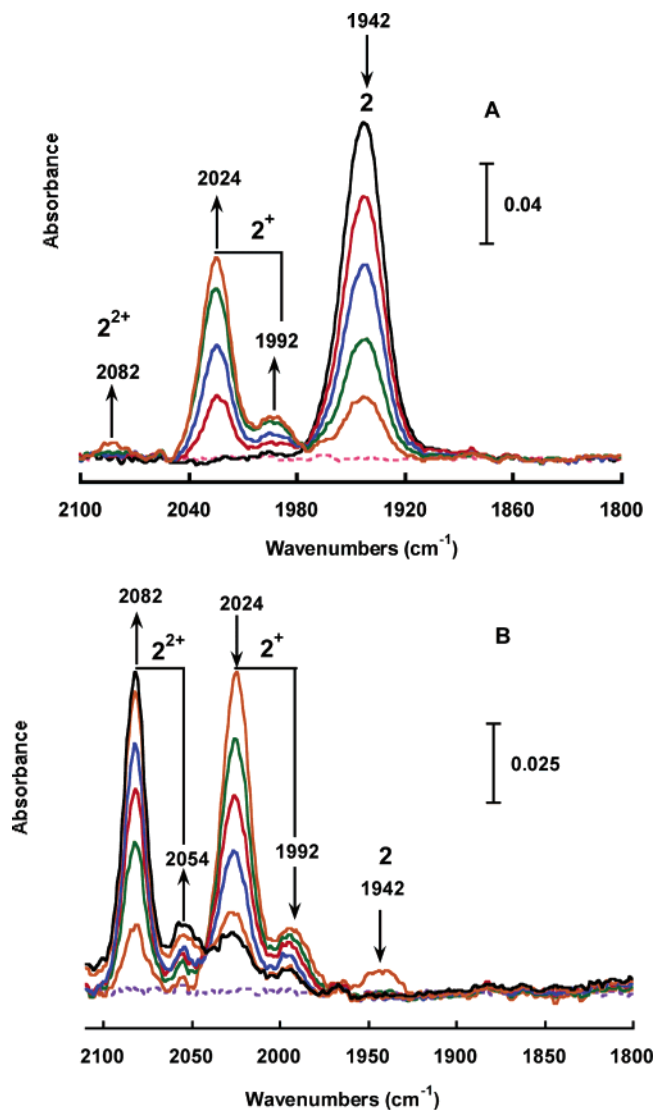
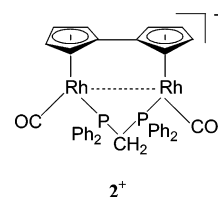


Figure 5. In-situ IR spectroelectrochemical monitoring of bulk oxidation of 0.5 mM **2** in $\text{CH}_2\text{Cl}_2/0.05 \text{ M} [\text{NBu}_4][\text{TFAB}]$ at $E_{\text{appl}} = -0.5 \text{ V vs Fc/Fc}^+$: (A) from beginning to passage of ca. 1 F/quiv; (B) continuing to passage of ca. 2 F/quiv.

($\Delta E_{1/2} \approx 90 \text{ mV}$).^{29,30} More importantly, information is obtained about the molecular and electronic structures of $\mathbf{2}^+$. The fact that the neutral complex **2** has a single ν_{CO} absorbance and the dication $\mathbf{2}^{2+}$ has two carbonyl absorptions is well understood based on known structures.³¹ That the monocation also has two carbonyl bands ($\nu_{\text{CO}} = 2024 \text{ cm}^{-1}$ (s), $\nu_{\text{CO}} = 1992 \text{ cm}^{-1}$ (w)) presents a strong argument in favor of the presence of a Rh–Rh bond in $\mathbf{2}^+$.



It is informative that the energetically less-shifted of the bands (at 1992 cm^{-1}) for $\mathbf{2}^+$ is still some 50 cm^{-1} higher in energy

(29) The conditions of the voltammetry results quoted in Table 1 (medium (vi)) and the IR experiment differ slightly in that the latter was performed at a supporting electrolyte concentration of 0.05 M and the temperature was 273 K.

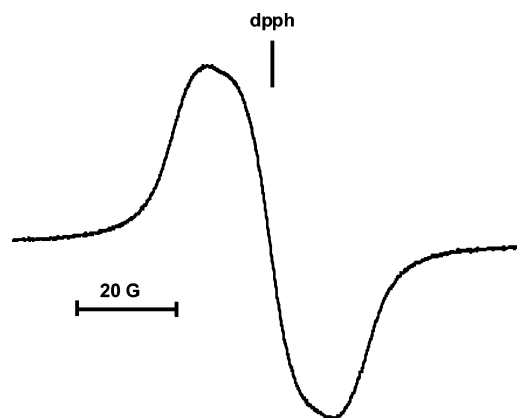


Figure 6. Fluid solution ESR spectra of 2^+ generated by chemical oxidation of **2** with 1 equiv of $[\text{FeCp}_2][\text{TFAB}]$ in CH_2Cl_2 at 273 K.

than the 1942 cm^{-1} band of **2**. On the basis of arguments made earlier on IR shifts in formally mixed-valence complexes,³⁰ the magnitude of this shift is indicative of strong electronic coupling between the two metals, strengthening support for metal–metal bond formation in 2^+ . It is also worth noting that shifts in ν_{CO} with the oxidation state of 2^{n+} track the overall change in molecular charge between $n = 0$ and either $n = 1+$ (larger shift, 81 cm^{-1} ; average 65 cm^{-1}) or $n = 2+$ (larger shift, 140 cm^{-1} , average 125 cm^{-1}).

Finally, a chemical oxidation^{16b} of **2** by 1 equiv of $[\text{FeCp}_2][\text{TFAB}]$ in CH_2Cl_2 was performed in order to approximate the electrochemical conditions and generate 2^+ for ESR purposes. A strong spectrum was obtained at both frozen (155 K) and fluid (room) temperatures. The former was approximately axial in shape with no detectable hyperfine splittings ($g_{\perp} = 2.035$, $g_{\parallel} = 1.990$, $g_{\text{av}} = 2.005$). The solution spectrum (Figure 6, $\langle g \rangle = 2.008$) displays inhomogeneous line broadening, indicating the presence of unresolved hyperfine interactions. Rhodium hyperfine splittings are inherently small owing to the rather small nuclear g -factor of ^{103}Rh .³²

II. Converting between Separate and Inverted Anodic Reactions of 3. IIA. Anodic Behavior of $\text{RhCp}(\text{COD})$. The redox-active component of $\text{Rh}_2\text{Fv}(\text{COD})_2$, **3**, is the $\text{Rh}(\text{C}_5\text{H}_4\text{R})$ -(COD) group. Anodic oxidation of the *mononuclear* parent $\text{RhCp}(\text{COD})$ has not, to our knowledge, been detailed in the literature.³³ In brief, we find the oxidation of $\text{RhCp}(\text{COD})$ to be a one-electron process of limited chemical reversibility, $E_{1/2} = 0.07\text{ V}$ vs ferrocene in $\text{CH}_2\text{Cl}_2/0.1\text{ M} [\text{NBu}_4][\text{PF}_6]$. Scan rates in excess of 10 V s^{-1} are necessary to see modest chemical reversibility at room temperature. Bulk electrolyses at 233 K passed slightly over 1 F/equiv, and the subsequent voltammetry scans showed an absence not only of $[\text{RhCp}(\text{COD})]^+$ but of other electroactive products as well. CV scans of $\text{RhCp}(\text{COD})$ in $\text{CH}_2\text{Cl}_2/0.1\text{ M} [\text{NBu}_4][\text{TFAB}]$ are very similar to those seen in the $[\text{PF}_6]^-$ electrolyte, making it unlikely that the electrolyte

(30) With very precise attention to both the coulometry and absorption values, along with assumptions concerning the absorptivity of either 2^+ or 2^{2+} relative to **2**, the value of K_{disp} could be determined directly from the spectroelectrochemical experiment. In the present case, this value is better determined from the measured $\Delta E_{1/2}$ values. See: Hill, M. G.; Rosenheim, L. D.; Mann, K. R.; Mu, X. H.; Schultz, F. A. *Inorg. Chem.* **1992**, *31*, 4108. Hill, M. G.; Mann, K. R. *Inorg. Chem.* **1991**, *30*, 1429.

(31) Even though the two CO ligands in 2^{2+} are chemically equivalent, the weak vibrational coupling referred to in ref 26 accounts for the observation of symmetric and asymmetric absorption bands.

(32) Weil, J. A.; Bolton, J. R.; Wertz, J. E. *Electron Paramagnetic Resonance*; John Wiley and Sons: New York, 1994; pp 535–536.

(33) Brief mention is made in: Winter, R.; Pierce, D. T.; Geiger, W. E.; Lynch, T. J. *J. Chem. Soc., Chem. Commun.* **1993**, 1949.

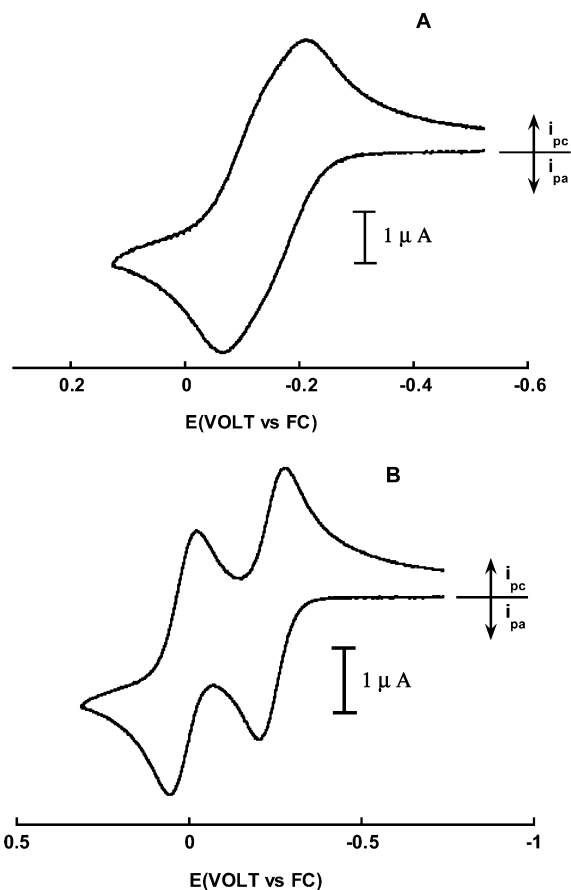


Figure 7. CV scans of 1 mM **3** in (A) $\text{CH}_2\text{Cl}_2/0.1\text{ M} [\text{NBu}_4][\text{PF}_6]$ and (B) $\text{CH}_2\text{Cl}_2/0.1\text{ M} [\text{NBu}_4][\text{TFAB}]$, scan rate 0.2 V/s , 1 mm GC disk electrode.

Table 2. Carbonyl-Region IR Energies for Different Oxidation States of $\text{Rh}_2\text{Fv}(\text{CO})_4$ (1**) and $\text{Rh}_2\text{Fv}(\text{CO})_2(\mu\text{-dppm})$ (**2**) in CH_2Cl_2**

compd or ion	ν_{CO} (cm^{-1})	av shift ^a (cm^{-1})	largest shift ^a (cm^{-1})
1	2038 (vs), 1978 (vs)	n.a.	n.a.
1 ⁺	2105 (vs), 2061 (vs), 2016 (w)	75	67
1 ²⁺	2153 (vs), 2123 (vs)	130	115
2	1942 (vs) ^b	n.a.	n.a.
2 ⁺	2024 (vs), 1992 (s)	65	82
2 ²⁺	2082 (vs), 2054 (s)	125	140

^a Largest shift = difference between highest energy ν_{CO} band and ν_{CO} of neutral compound; av shift = average difference between energies of two ν_{CO} bands and that of neutral compound. The weak band is not used to compute the average shift of **1**⁺. ^b Relative intensity designations: vs = very strong, s = strong, w = weak.

anion plays a role in the follow-up reaction. Loss of the COD ligand is likely responsible for the limited longevity of $[\text{RhCp}(\text{COD})]^+$ and, by inference, of **3**⁺. As shown below, the primary oxidation products of **3**, while still subject to slow decomposition, are sufficiently long-lived to allow investigation of medium effects and, ultimately, the characterization of the one-electron product **3**⁺ by ESR spectroscopy.

IIB. Anodic Oxidation of $\text{Rh}_2\text{Fv}(\text{COD})_2$ in Media Containing Traditional Anions. The oxidation of **3** proceeds through two unresolved one-electron waves in $\text{CH}_2\text{Cl}_2/[\text{NBu}_4][\text{PF}_6]$ (Figure 7A) having $\Delta E_{1/2} \approx 60\text{ mV}$ (digital simulations,³⁴ Table 3). The resulting K_{disp} of 0.095 means that under these conditions **3**⁺ makes up roughly 60% of the equilibrium mixture of the three oxidation states of $\text{Rh}_2\text{Fv}(\text{COD})_2$. Manipulation of the $\Delta E_{1/2}$ value was approached with the objective of finding conditions in which there is either (i) a significant increase in

Table 3. $E_{1/2}$ Values (volt vs ferrocene) for $M_2Fv(COD)_2$, $M = Rh$ (**3**) and $M = Co$ (**4**), TFAB = $[B(C_6F_5)_4]^-$, $BArF_{24} = [B(C_6H_3(CF_3)_2)_4]^-$

solvent	supporting electrolyte ^a	cmpd	$E_{1/2}(1)^b$	$E_{1/2}(2)^c$	$\Delta E_{1/2}$ (mV)	$\log K_{disp}$
CH ₂ Cl ₂	[NBu ₄][BArF ₂₄]	3	-0.25	0.03	280	-4.73
CH ₂ Cl ₂	[NBu ₄][TFAB]	3	-0.24	0.02	270	-4.57
CH ₂ Cl ₂	[NBu ₄][PF ₆]	3	-0.17	-0.11	60	-1.02
glyme	[NBu ₄][TFAB]	3	-0.14	-0.04	100	-1.69
glyme	[NBu ₄][PF ₆]	3	-0.11	-0.16	-50	0.85
Et ₂ O	[NBu ₄][BArF ₂₄]	3	-0.19	0.07	260	-4.40
CH ₂ Cl ₂	[NBu ₄][PF ₆]	RhCp (COD)	-0.07	n.a.		
CH ₂ Cl ₂	[NBu ₄][PF ₆] ^d	4	-0.30	-0.07	230	-3.89
CH ₂ Cl ₂	[NBu ₄][TFAB]	4	-0.34	+0.06	400	-6.76

^a 0.10 M. ^b One-electron oxidation of neutral compound. ^c One-electron oxidation of monocation. ^d Remeasurement. See ref 38 for original report.

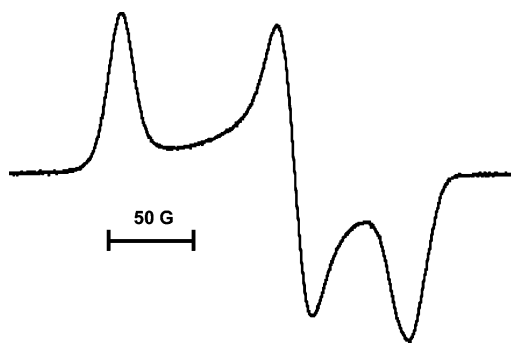


Figure 8. Frozen-solution ESR spectrum of 3^+ at 163 K, generated by bulk oxidation of 0.6 mM **3** in CH₂Cl₂/0.05 M [NBu₄][TFAB], $E_{appl} = -0.1$ V, $T = 273$ K.

$\Delta E_{1/2}$, thereby more strongly favoring 3^+ , or (ii) sufficient decrease in $\Delta E_{1/2}$ to achieve potential inversion and a single two-electron wave for $3/3^{2+}$. Using the integrated approach to medium effects,⁷ we employed a WCA to accomplish the former and a stronger donor solvent to achieve the latter. $\Delta E_{1/2}$ changes of up to 330 mV were observed through these manipulations. No discernible change in either chemical or electrochemical reversibility was seen on a voltammetric time scale.

IIc. Increasing $\Delta E_{1/2}$ to Favor 3^+ . Replacement of $[PF_6]^-$ by either of the more weakly ion-pairing anions TFAB or BArF₂₄ resulted in an increase of over 200 mV in $\Delta E_{1/2}$ and separate waves due to $3/3^+$ and $3^+/3^{2+}$ were observed (Figure 7B). A bulk electrolysis carried out at $E_{appl} = -0.1$ V in CH₂Cl₂/0.05 M [NBu₄][TFAB] at 273 K was halted after release of approximately 0.95 F/equiv. The solution was probed by voltammetry, after which a sample was removed for ESR spectroscopy. Some decomposition of oxidized **3** accompanied the electrolysis,³⁵ but comparison of LSV peak heights showed that there was a substantial (ca. 40%) yield of 3^+ . The frozen-glass ESR spectrum of this sample (Figure 8) showed one clean rhombic-shaped signal ($g_1 = 2.1116$, $g_2 = 2.0434$, $g_3 = 2.0005$) attributed to 3^+ .

IIId. Decreasing $\Delta E_{1/2}$ to Disfavor 3^+ : Toward Inverted Potentials. Starting from the makeup of the medium CH₂Cl₂/[NBu₄][TFAB] (low donor solvent/weakly interacting anion), there are two options available for decreasing the $\Delta E_{1/2}$ of 270 mV, one of which, namely, the addition of a stronger ion-pairing

(34) Specific conditions were as follows: electrolyte concentration 0.075 M; scan rate 200 mV s⁻¹, 1.5 mm diameter glassy carbon electrode; simulation k_s and α values of 0.08 cm s⁻¹ and 0.5, respectively, for both one-electron couples. Digital simulation of data taken under somewhat different conditions gave the similar result of $\Delta E_{1/2} = 70$ mV. Those conditions were as follows: electrolyte concentration 0.10 M; scan rate 100 mV s⁻¹; 1.0 mm diameter Pt electrode; k_s and α values of 0.1 cm s⁻¹ and 0.5, respectively.

(35) CV peaks for follow-up products were seen at $E_{1/2} = -0.28$ V (rev) and $E_{pc} = -1.65$ V (irrev), along with a smaller cathodic peak at $E_{pc} = -1.12$ V (irrev).

anion, is obvious from previous discussions. The second involves using a solvent of greater donor ability, which serves to thermodynamically stabilize more positively charged products.⁷ To take full advantage of the change in donor strength, the dielectric constant of the new solvent must remain low ($\epsilon < 10$) in order to retain strong ion-pairing effects.

The solvent effect can be quite large, as shown by comparison of the $\Delta E_{1/2}$ values for **3** in two solvents of similar dielectric constants but substantially different donor numbers. When the electrolyte anion is TFAB, the $\Delta E_{1/2}$ value decreases from 270 mV in CH₂Cl₂ ($\epsilon = 8.9$, donor number = 0) to 100 mV in 1,2-dimethoxyethane (glyme, $\epsilon = 7.2$, donor number = 20)³⁶ (Table 3). A additional change of -150 mV for the $\Delta E_{1/2}$ value in glyme is achieved by replacement of TFAB by $[PF_6]^-$, resulting in an overall reduction in $\Delta E_{1/2}$ of -320 mV on going from CH₂Cl₂/TFAB to glyme/ $[PF_6]^-$. In Figure 9, these effects are demonstrated visually by square-wave voltammetry. Addition of 250 equiv of $[PF_6]^-$ to an original CH₂Cl₂/[NBu₄][TFAB] solution containing 0.6 mM **3** is shown to decrease $\Delta E_{1/2}$ by about 140 mV (Figure 9B vs 9A). Stepwise addition of glyme at this point further decreases $\Delta E_{1/2}$ until a symmetric wave is seen (Figure 9F), denoting a single two-electron wave in 1:1 CH₂Cl₂/glyme. From the breadth of the wave in Figure 9F (90 mV at half-height), a $\Delta E_{1/2}$ value of +35 mV is obtained.³⁷ In a pure glyme solution containing 0.15 M [NBu₄][PF₆], the experimental square-wave width of 53 mV gives $\Delta E_{1/2} = -50$ mV. This value was confirmed by the width of the DPV peak, and digital simulations of CV scans over the scan-rate range of 0.2 to 1 V s⁻¹ (Figure 10 and Figure SM1 in the Supporting Information) allowed the final assignment of $E_{1/2}(1) = -0.11$ V and $E_{1/2}(2) = -0.16$ V. Potential inversion is realized under these conditions.

We note finally the $\Delta E_{1/2}$ value of 260 mV, observed in diethyl ether ($\epsilon = 4.2$, donor number = 19.2) containing 0.05 M [NBu₄][BArF₂₄], which seems surprisingly large considering the strong donor ability of Et₂O compared to CH₂Cl₂, in which essentially the same value is measured. Proper delineation of this effect will require a better understanding of anodic processes in acyclic ether solvents, measurements that are now feasible owing to the increased solubilities and conductivities of WCA-based electrolytes in these solvents.

III. Confirmation of 1:2 Ion Pairing for $[3]^{2+}:[PF_6]^-$. Stepwise addition of $[PF_6]^-$ to a solution of **3** in CH₂Cl₂/[NBu₄][TFAB] made possible a plot of the change in $\Delta E_{1/2}$ (i.e., $\Delta\Delta E_{1/2}$) versus log concentration of $[PF_6]^-$ (Figure SM2, Supporting Information). At high concentrations a linear relationship is apparent having a slope of 107 mV, in reasonable

(36) Solvent parameters were taken from Linert, W.; Fukuda, Y.; Camard, A. *Coord. Chem. Rev.* **2001**, *218*, 113.

(37) This value was actually obtained from the width of the DPV wave, using a working curve constructed from the data of ref 19. The DPV and SWV peak shapes are very similar for Nernstian systems.

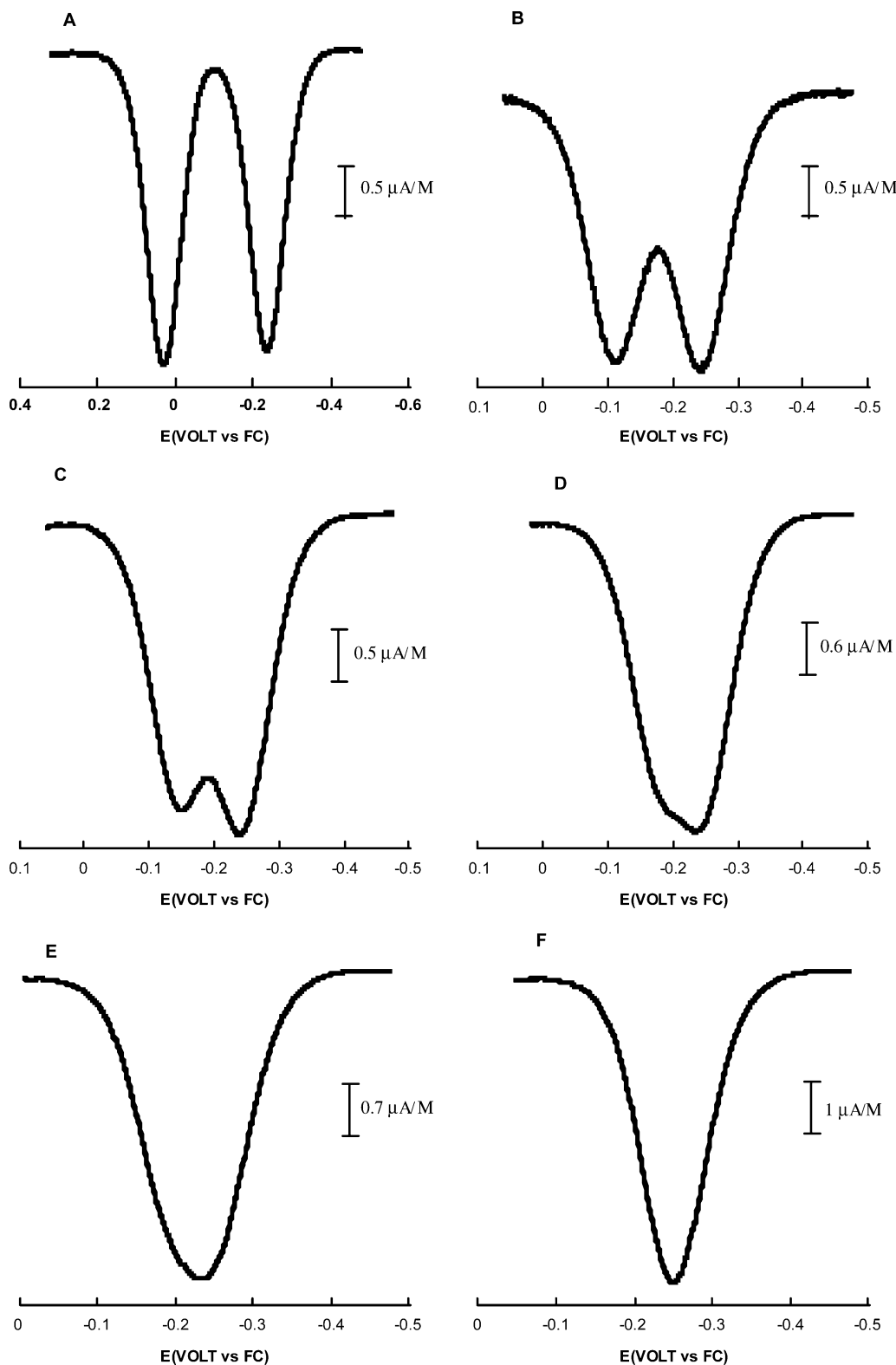
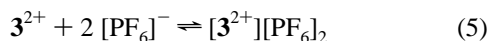


Figure 9. Square-wave voltammograms (frequency 10 Hz, pulse height 25 mV) of 0.6 mM **3** at 1 mm GC disk in (A) $\text{CH}_2\text{Cl}_2/0.1 \text{ M } [\text{NBu}_4][\text{TFAB}]$, (B) $\text{CH}_2\text{Cl}_2/0.1 \text{ M } [\text{NBu}_4][\text{TFAB}] + 250 \text{ equiv of } [\text{NBu}_4][\text{PF}_6]$, (C) solvent mixture $\text{CH}_2\text{Cl}_2/\text{glyme}$ (90:10% v/v) + 0.1 M $[\text{NBu}_4][\text{TFAB}]$ and 250 equiv of $[\text{NBu}_4][\text{PF}_6]$, (D) $\text{CH}_2\text{Cl}_2/\text{glyme}$ (80:20% v/v) + 0.1 M $[\text{NBu}_4][\text{TFAB}]$ and 250 equiv of $[\text{NBu}_4][\text{PF}_6]$, (E) $\text{CH}_2\text{Cl}_2/\text{glyme}$ (60:40% v/v) + 0.1 M $[\text{NBu}_4][\text{TFAB}]$ and 250 equiv of $[\text{NBu}_4][\text{PF}_6]$, (F) $\text{CH}_2\text{Cl}_2/\text{glyme}$ (50:50% v/v) + 0.1 M $[\text{NBu}_4][\text{TFAB}]$ and 250 equiv of $[\text{NBu}_4][\text{PF}_6]$; y-axis is concentration-normalized current.

agreement with the value of 118 mV expected if the dominant ion-pairing interaction of 3^{2+} is with two $[\text{PF}_6]^-$ anions, as given in eq 5:



Measurements of $\Delta\Delta E_{1/2}$ values accompanying changes in ion-pairing agents hold, in principle,^{2d} information about the equilibrium constants of eq 5 as well as those involving the ion-pairs $[3^+][\text{PF}_6]$ and $\{[3^{2+}][\text{PF}_6]\}^+$, but the present data are insufficient to address the complexity of the analysis.

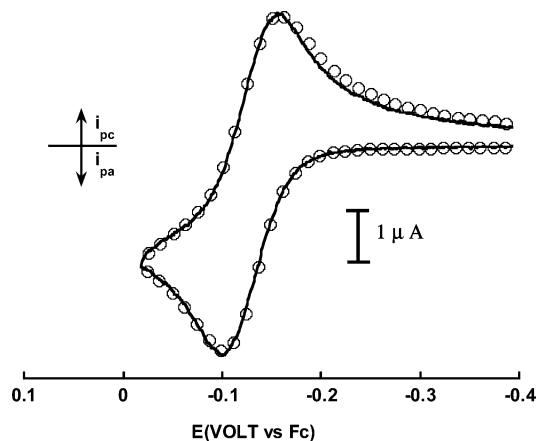


Figure 10. Experimental (solid line) and simulated (circles) CV scans of 0.3 mM **3** in glyme/0.15 M [NBu₄][PF₆] at 1 mm GC disk, scan rate 1 V s⁻¹. Relevant simulation parameters: $E_{1/2}(1) = -0.11$ V, $k_s^1 = 8 \times 10^{-2}$ cm s⁻¹, $\alpha^1 = 0.5$; $E_{1/2}(2) = -0.16$ V, $k_s^2 = 5.5 \times 10^{-2}$ cm s⁻¹, $\alpha^2 = 0.5$; $D_0(\mathbf{3}) = D_0(\mathbf{3}^+) = 6.7 \times 10^{-6}$ cm s⁻¹; $D_0(\mathbf{3}^{2+}) = 4.7 \times 10^{-6}$ cm s⁻¹; capacitance = 5×10^{-8} F cm⁻²; electrode area = 0.0079 cm².

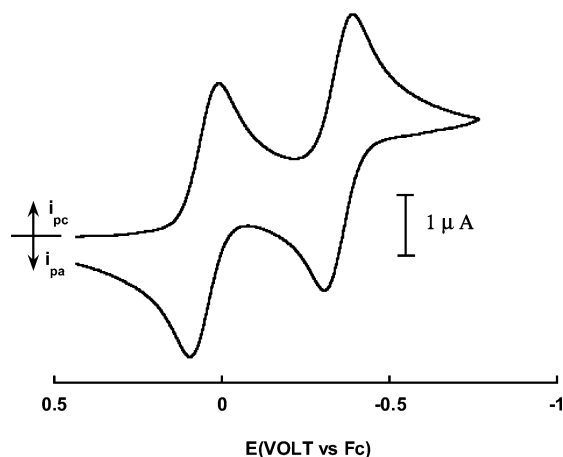


Figure 11. CV (0.1 V s⁻¹, 1 mm glassy carbon disk) of the dication **4**²⁺ formed after bulk electrolysis of 1 mM **4** in CH₂Cl₂/0.05 M [NBu₄][TFAB] at $E_{\text{appl}} = 0.45$ V. The fact that the current is zero at the rest potential (ca. 0.45 V) is consistent with exhaustive anodic oxidation of the neutral starting material.

III. Oxidation of 4 under WCA Conditions. For the sake of comparison with the dirhodium compound **3**, the anodic reactions of the dicobalt analog $\text{Co}_2\text{Fv}(\text{COD})_2$, **4**, were carried out in CH₂Cl₂/0.1 M [NBu₄][TFAB] (a full paper on the oxidation of **4** in CH₂Cl₂/0.1 M [NBu₄][PF₆] has been published³⁸). As expected, the $\Delta E_{1/2}$ value increased (from 230 mV to 400 mV) as [PF₆]⁻ was replaced by TFAB. Furthermore, the oxidation products were noticeably more persistent. Room-temperature bulk electrolysis at increasing values of E_{appl} produced, first, the dark green monocation **4**⁺ and, then, the deep blue dication **4**²⁺ with no evidence of decomposition (see Figure 11 for CV of **4**²⁺).³⁹ Note that in Figure 11 the current at the rest potential is essentially zero, showing that the original neutral compound had been completely converted to the corresponding dication. LSV scans confirmed this quantitatively. Cathodic back-electrolysis quantitatively regenerated neutral **4**. The oxidized species **4**⁺ and **4**²⁺ join the growing number of organometallic radical cations and multicharged cations that

exhibit increased kinetic stabilities when generated in the presence of WCA anions.^{9–12,40,41}

Discussion

The $\Delta\Delta E_{1/2}$ values for **3** and **4** in dichloromethane increase by 220 and 170 mV, respectively, when the supporting electrolyte anion is changed from [PF₆]⁻ to TFAB or BArF₂₄⁻. These values are in concert with the previously reported $\Delta\Delta E_{1/2}$ value of +190 mV reported for biferrocene under these conditions.⁴¹ It seems reasonable to conclude that an electrolyte anion effect (WCA vs traditional anion) of ca. +200 mV in $\Delta\Delta E$ is characteristic of dinuclear fulvalenediyl complexes having positively charged redox products. This electrolyte change imparts a decrease of over 10³ in K_{disp} to the disproportionation of the one-electron product.⁴² It should be noted that the estimate of ca. +200 mV pertains to solutions having a [NBu₄]⁺ cation, and those employing more strongly ion-pairing electrolyte cations, e.g., [NEt₄]⁺ or Na⁺, will result in further increases in $\Delta\Delta E_{1/2}$. The consequent thermodynamic stabilization of the one-electron product provides a welcome option for studies of class II⁴³ mixed-valent systems. In the present case, this medium effect allowed for the facile spectral characterization of **3**⁺.

The $\Delta\Delta E_{1/2}$ values for **1** and **2**, while qualitatively consistent with the above model, require a more complex analysis. Although the change of +220 mV for **1** on going from [PF₆]⁻ to TFAB is consistent with the findings for **3**, **4**, and biferrocene, the *trans*-to-*cis* reorientation and subsequent formation of a Rh–Rh bond in the oxidation of **1** has an unknown quantitative effect on the $\Delta\Delta E_{1/2}$ value.⁴⁴ Also, the smaller $\Delta\Delta E$ value of +110 mV for the anion effect on **2** may be influenced by making and breaking of the Rh–Rh bond in the redox processes. From a utilitarian viewpoint, the increased $\Delta E_{1/2}$ for **2** made possible the spectral characterization of **2**⁺. However, further studies will be required to address the question of whether medium effects are substantially different for redox processes that include major structural changes.⁴⁵

Systematic alterations of *both* the solvent and the electrolyte allow even more powerful manipulations of $\Delta E_{1/2}$, as shown by the 330 mV shift for compound **3** as the medium was changed from CH₂Cl₂/[NBu₄][BArF₂₄] to glyme/[NBu₄][PF₆]. It is noteworthy that an inverted $\Delta E_{1/2}$ is made possible for **3**/**3**²⁺ even though this redox pair does not appear to have the capacity for a structural change of the magnitude ordinarily associated with potential-inverted two-electron processes.^{2c,d,3e,46} The large preferential stabilization of the **3**⁺/**3**²⁺ couple (compared to **3**/**3**⁺) must arise primarily from increases of both ion-pairing and solvation of the dication **3**²⁺ by [PF₆]⁻ and glyme, respectively.

In terms of new data on systems previously studied under traditional electrolyte conditions,¹⁴ it is the spectral characteriza-

(40) Camire, N.; Nafady, A.; Geiger, W. E. *J. Am. Chem. Soc.* **2002**, *124*, 7260.

(41) Camire, N.; Mueller-Westerhoff, U. T.; Geiger, W. E. *J. Organomet. Chem.* **2001**, *637–639*, 823.

(42) At 298 K, $\log K_{\text{disp}} = 16.92\Delta E^\circ$, where ΔE° is in volts.

(43) Robin, M. B.; Day, P. *Adv. Inorg. Chem. Radiochem.* **1967**, *10*, 247.

(44) Note also that the $\Delta E_{1/2}$ value of -140 mV for **1** in [NBu₄][PF₆] is only an estimated value, based on digital simulations of a quasi-reversible electron-transfer system having inverted $E_{1/2}$ potentials. See ref 14 for details.

(45) Solvation energies, in particular, can be expected to be affected by some types of structural changes.

(46) For some leading references see: Stoll, M. E.; Belanzoni, P.; Calhorda, M. J.; Drew, M. G. B.; Félix, V.; Geiger, W. E.; Gamelas, C. A.; Gonçalves, I. S.; Romão, C. C.; Veiros, L. F. *J. Am. Chem. Soc.* **2001**, *123*, 10595.

(38) Chin, T. T.; Geiger, W. E. *Organometallics* **1995**, *14*, 1316.

(39) Only a 40% yield of **4**²⁺ was reported in ref 38 using [PF₆]⁻ as the electrolyte anion, even at the considerably reduced temperature of 243 K.

tion of the one-electron intermediates $\mathbf{1}^+$ and $\mathbf{2}^+$ that stands out. The IR spectra of $\mathbf{1}^+$ and $\mathbf{2}^+$ confirm the presence of the previously postulated Rh–Rh bonds in these radicals.

Acknowledgment. This work was supported at the University of Vermont by the National Science Foundation (CHE-0092702 and CHE-041703).

Supporting Information Available: Two figures showing (SM1) simulations of the CV scans of $\mathbf{3}$ at different scan rates and (SM2) a plot of $\Delta\Delta E_{1/2}$ vs $\log [\text{PF}_6]^-$ in high concentration range for compound $\mathbf{3}$ in $\text{CH}_2\text{Cl}_2/[\text{NBu}_4][\text{TFAB}]$ to which $[\text{PF}_6]^-$ is being added. This material is available free of charge through the Internet at <http://pubs.acs.org>.

OM051101E